AIP | Applied Physics Letters

Refractive-index-based optofluidic particle manipulation

Kang Soo Lee, Kyung Heon Lee, Sang Bok Kim, Jin Ho Jung, Byung Hang Ha, Hyung Jin Sung, and Sang Soo Kim

Citation: Applied Physics Letters **103**, 073701 (2013); doi: 10.1063/1.4817938
View online: http://dx.doi.org/10.1063/1.4817938
View Table of Contents: http://scitation.aip.org/content/aip/journal/apl/103/7?ver=pdfcov
Published by the AIP Publishing

Refractive-index-based optofluidic particle manipulation

Kang Soo Lee, Kyung Heon Lee, Sang Bok Kim, Jin Ho Jung, Byung Hang Ha, Hyung Jin Sung,[a] and Sang Soo Kim[a]
Department of Mechanical Engineering, KAIST 291 Daehak-ro, Yuseong-gu, Daejeon 305-701, South Korea

(Received 21 March 2013; accepted 23 July 2013; published online 13 August 2013)

This letter describes optofluidic particle manipulation based on the refractive index contrast between the particle and the surrounding medium. A laser beam propagated along one sidewall of a microfluidic channel will introduce a force that pushes a high-refractive-index particle toward the Gaussian-shaped laser beam center axis. By contrast, a low-refractive-index particle will be pushed away from the beam center axis and toward the other sidewall of the channel because the direction of the gradient forces acting on such a particle is opposite the direction of the forces acting on a high-refractive-index particle. The gradient forces acting on a particle were calculated to predict and interpret the particle behavior. High-refractive-index and low-refractive-index particles, prepared from polystyrene latex (PSL) and hollow glass particles with refractive indices of 1.59 and 1.22, respectively, were employed. The PSL and hollow glass particles could be separated based on their refractive indices. Doubly attached identical particles behaved as a single particle.
 [http://dx.doi.org/10.1063/1.4817938]

The field of optofluidics, which encompasses the combined research fields of optics and fluidics, has been applied toward the development of a variety of applications, such as physical instruments (e.g., optofluidic microscopy), chemical sensors (e.g., optofluidic surface-enhanced Raman spectroscopy (SERS)), and energy conversion (e.g., optofluidic biofuel production *via* photosynthesis).[1–3] Optical particle manipulation is one of the most widely studied optofluidic technologies with applications in the fields of biology, diagnostics, and genetics. Since the first demonstration of the phenomenon of optical levitation using an optical force,[4] optical particle manipulation applications have expanded into a variety of research fields, including optofluidic particle separation, laser scissors, laser tweezer, photon-driven micromotors, laser nanoaxotomy, and others.[5–10] The technique has several advantages over alternative particle or cell manipulation techniques (e.g., based on electrophoretic, magnetophoretic, hydrophoretic, structural, and particle characteristics): optofluidic techniques are facile with respect to single particle/cell manipulation, independent of the charge state of either the particle or the surrounding medium, and negligibly impact the cell viability. Radiation forces consist of two force components: a scattering force (parallel to the propagation direction) and a gradient force (toward the maximum or minimum intensity of the illumination beam). The characteristics of optical particle manipulation depend mainly on the refractive index and the size of a particle. Research into optical particle manipulation has focused on these parameters.[11,12] The optical mobility is a parameter that accounts for the effects of both the refractive index and the particle size. Particles with different sizes and refractive indices can display comparable optical mobilities, leading to similar separation characteristics.[13] Therefore, particle manipulation must be performed in such a way as to depend on a single parameter.[10]

The present study examined a refractive-index-driven particle manipulation technique in a laser beam system. The gradient force was used as a driving force in a continuous separation strategy. Particles with refractive indices either higher (high-refractive-index) or lower (low-refractive-index) than the refractive index of the surrounding medium were separated due to the opposite directions of the gradient forces acting on them. The gradient forces acting on the high-refractive-index and low-refractive-index particles were calculated to predict and interpret the particle behavior in the system.

Figure 1 shows a schematic diagram of the experimental setup. A continuous wave neodymium-doped yttrium aluminum garnet (CW Nd:YAG) laser (wavelength = 532 nm) was employed as an illumination beam. The size of the laser beam was expanded using a beam expander (3×), and the beam was subsequently focused using a lens with a minimum beam waist of 7 μm. A light emitting diode (LED) was

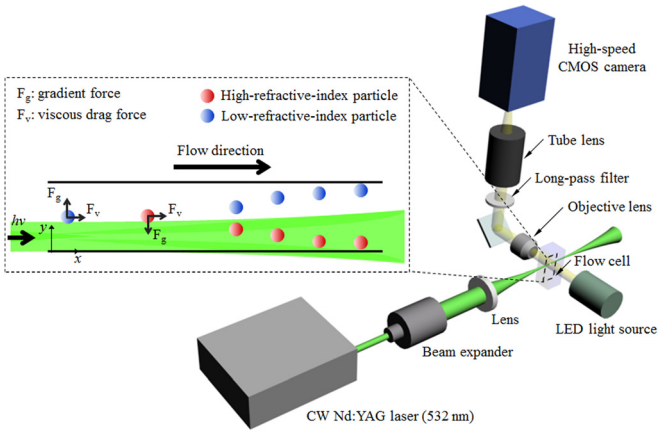

FIG. 1. Schematic diagram of the experimental setup. The laser wavelength was 532 nm. The inset shows the principle underlying the present optofluidic particle manipulation system. The laser beam center axis was aligned adjacent and parallel to the sidewall of the microfluidic channel.

[a]Authors to whom correspondence should be addressed. Electronic addresses: hjsung@kaist.ac.kr and sskim@kaist.ac.kr

used as a light source for visualization. Images were obtained using a high-speed complementary metal oxide semiconductor (CMOS) camera (pco. 1200 hs, PCO). To prevent damage to the camera *via* scattering of the laser beam, a long pass filter (cut-off wavelength = 575 nm) was inserted between the flow cell and the camera. Polydimethylsiloxane (PDMS) microfluidic channels, which ensure the optical transparency, with single inlet and outlet were fabricated using a soft-lithography process and O_2 plasma bonding. The width and height of the channel were 20 μm and 26 μm, respectively. A facet smoothing technique was used to prevent laser beam scattering at the channel sidewall.[14,15] Deionized (DI) water ($n = 1.33$) was used as a working fluid. The inset illustrates the principles underlying particle manipulation in the system. The laser beam propagates in the direction of the liquid flow. The laser beam center axis was aligned adjacent and parallel to a sidewall in the microfluidic channel. A high-refractive-index particle entering the influence region of the laser beam was pushed toward the laser beam center axis due to the positive gradient force, whereas a low-refractive-index particle was deflected toward the opposite sidewall of the channel due to the negative gradient force. A polystyrene latex (PSL) particle ($n = 1.59$, Duke Scientific Corp.) and a hollow glass particle ($n \approx 1.22$, Polyscience, Inc.) were used as the high-refractive-index and low-refractive-index particles, respectively.

Figure 2 shows the gradient force acting on the PSL and hollow glass particles under various laser beam powers in DI water. Since the present study deals with micron-sized particles (~5 μm), the photon stream method was employed to calculate the radiation forces.[16] An analytical expression for the gradient force on a sphere is derived by the photon stream method[16]

$$F_g = -\frac{1}{2c}\int_0^{2\pi}\int_0^{\pi/2} I(\rho,x)[n(\rho)R(\rho)\sin 2\theta_1 - n(\rho')T(\rho)T(\rho')\sin(\theta_1 - 2\theta_2 + \theta_3)]r_p^2 \sin 2\theta_1 \cos\varphi d\theta_1 d\varphi, \quad (1)$$

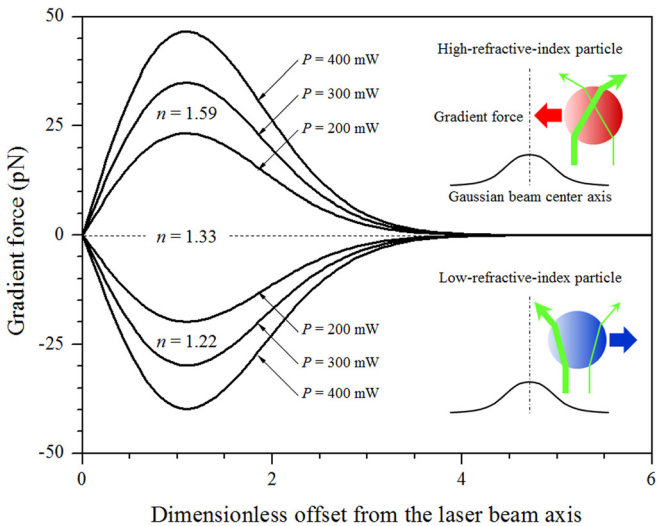

FIG. 2. The gradient force acting on PSL (high-refractive-index) and hollow glass (low-refractive-index) particles under various laser beam powers. The inset illustrates the principles underlying the positive and negative gradient forces.

where c is the speed of light in free space. $I(\rho, x)$ is the beam intensity, which is assumed to have a Gaussian cross-sectional profile in the present study. ρ and x are the radial distance from the Gaussian beam center axis and the axial distance from the position of the minimum beam waist, respectively. $n(\rho)$ and $n(\rho')$ denote the refractive indices of the surrounding medium at the first and second interfaces where the photons meet in the particle, respectively. θ_1, θ_2, and θ_3 are the incident angle of a photon at the first interface, the refraction angle at the first interface, and the refraction angle at the second interface, respectively. R and T are the Fresnel reflectance and transmittance, respectively. r_p is the particle radius and φ is the polar angle between the direction of the radial component of the momentum and the radial direction. The dimensionless radial offset, parameter corresponding to the x-axis in Fig. 2, is the distance between the beam center axis and the particle center, divided by the particle radius. As shown in Fig. 2, the high-refractive-index particle experienced a positive gradient force to the Gaussian-shaped beam center axis, whereas a negative gradient force to the minimum beam intensity acted on the low-refractive-index particle. As a result, the high-refractive-index particle, initially positioned away from the laser beam center axis, was pushed toward the beam axis, whereas the low-refractive-index particle at the same initial position was pushed away from the beam center axis. The magnitude of the gradient force increased with the laser beam power. The principles underlying the positive and negative gradient forces are illustrated in the insets in Fig. 2. A photon impinging on the first interface between the high-refractive-index particle, and the surrounding medium is refracted with an angle smaller than the incident angle, as described by Snell's law

$$n_1 \sin\theta_1 = n_2 \sin\theta_2. \quad (2)$$

On the other hand, the opposite is true for a low-refractive-index particle. The number of photons passing through the particle is intense at the beam center axis and decreases as the radial offset increases due to the Gaussian cross-section of the laser beam. The net force resulting from the momentum change in the photons is directed either inward toward the beam axis or outward away from the beam axis, for high-refractive-index or low-refractive-index particles, respectively.

Figure 3 shows the trajectory of a PSL (high-refractive-index) particle. The particle velocity was approximately

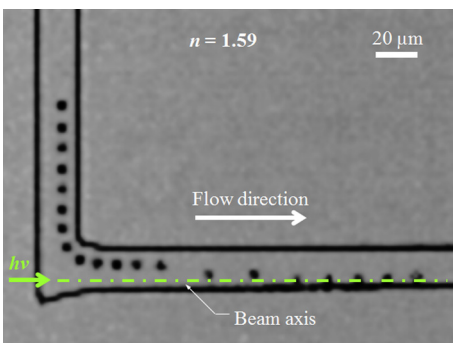

FIG. 3. Trajectories of a PSL (high-refractive-index) particle (enhanced online) [URL: http://dx.doi.org/10.1063/1.4817938.1].

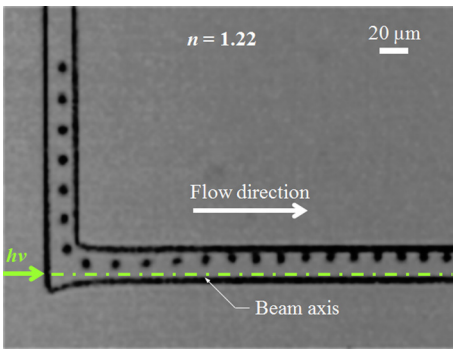

FIG. 4. Trajectories of a hollow glass (low-refractive-index) particle (enhanced online) [URL: http://dx.doi.org/10.1063/1.4817938.2].

270 μm/s and the illumination laser beam power was 426 mW at the source outlet. The time interval between adjacent particles in the snapshot was 50 ms. The direction of the laser beam propagation coincides with the flow direction. As a particle entered the region of influence of the laser beam, it was pushed toward the center axis of the illumination beam under a positive gradient force. Furthermore, the scattering force, which acted parallel to the flow direction, accelerated the particle along the fluid stream.

Figure 4 shows the trajectories of a hollow glass (low-refractive-index) particle. The particle velocity was approximately 1 mm/s and the laser beam power was 194 mW. The time interval between adjacent particles in the snapshot was 20 ms. The particles were deflected away from the beam center axis due to the negative gradient force. In contrast with the case of the high-refractive-index particle, the particle acceleration along the flow direction due to the scattering force was negligible. Although most techniques that employ loosely focused laser beams function only under limited low particle velocities (on the order of hundreds of μm/s), the present system could be operated at speeds up to mm/s because the flow and beam propagation directions were the same. The optical force on a particle was not found to affect the behaviors of other particle downstream, as demonstrated using a stream of hollow glass particles flowing in a row (see Movie S1 in supplementary materials[17]). We observed that once a particle had been separated at the entrance region according to its refractive index, it travelled along the flow direction without interacting with the beam or the subsequent particles.

Figure 5 shows the trajectories of doubly attached hollow glass particles. The particle velocity was about 580 μm/s and the laser power was 437 mW. The time interval between adjacent particles in the snapshot was 70 ms. In a particle separation system, the particles inserted into the influence region of the illumination beam are usually attached together in aggregates. As shown in Fig. 5, the motions of these aggregates were similar to the motions of a single particle, possibly because particles near the laser beam axis dragged the other particles along under the higher gradient force. Hence, a cluster of particles behaves as a single big particle. We also observed that doubly attached PSL particles behaved as a single particle. Future work will focus on numerical and experimental analyses of the motions of aggregates prepared by attaching one PSL particle and one hollow glass particle together.

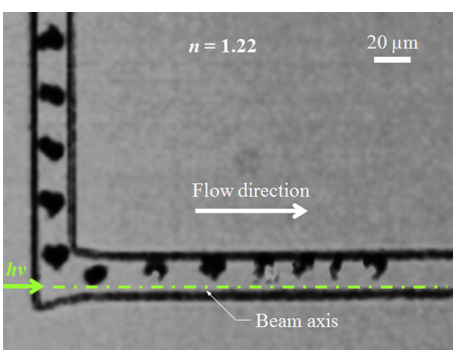

FIG. 5. Trajectories of the doubly attached hollow glass particles (enhanced online) [URL: http://dx.doi.org/10.1063/1.4817938.3].

In summary, optofluidic particle manipulation, based on the refractive indices of the particles, was demonstrated using a single working fluid, DI water. Particle separation was achieved in a microfluidic laser beam system with a relatively low laser power (~hundreds of mW) and at a high flow velocity (up to thousands of μm/s). PSL and hollow glass particles were used as the high-refractive-index and low-refractive-index particles, respectively. The particle behaviors were modeled and interpreted in terms of the gradient forces acting on the PSL and hollow glass particles. The gradient forces acting on these particles were opposite in sign. As a result, PSL particles were pushed toward the laser beam center axis, whereas hollow glass particles were deflected toward the opposite sidewall of the channel. Doubly attached identical particles behaved as a single particle. The present system is expected to be applicable to continuous refractive index driven biological particle manipulation,[18] micro bubble removal from the microfluidic cell culture array, and cell manipulation by controlling the refractive index of the surrounding medium.

This work was supported by the Creative Research Initiatives (No. 2013-003364) program of the National Research Foundation of Korea (MSIP).

[1]O. Mudanyali, E. Mcleod, W. Luo, A. Greenbaum, A. F. Coskun, Y. Hennequin, C. P. Allier, and A. Ozcan, Nat. Photonics **7**, 247 (2013).
[2]P. Measor, L. Seballos, D. Yin, Z. Zhang, E. J. Lunt, A. R. Hawkins, and H. Schmidt, Appl. Phys. Lett. **90**, 211107 (2007).
[3]M. D. Ooms, V. J. Sieben, S. C. Pierobon, E. E. Jung, M. Kalontarov, D. Erickson, and D. Erickson, Phys. Chem. Chem. Phys. **14**, 4817 (2012).
[4]A. Ashkin, Phys. Rev. Lett. **24**, 156 (1970).
[5]S. X. Guo, F. bourgeois, T. Chokshi, N. J. Durr, M. A. Hilliard, N. Chronis, and A. B. Yakar, Nat. Method **5**, 531 (2008).
[6]T. Wu, T. A. Nieminen, S. Mohanty, J. Miotke, R. L. Meyer, H. R. Dunlop, and M. W. Berns, Nat. Photonics **6**, 62 (2012).
[7]M. W. Bern, Sci. Am. **278**, 62 (1998).
[8]K. S. Lee, S. Y. Yoon, S. B. Kim, K. H. Lee, H. J. Sung, and S. S. Kim, Microfluid. Nanofluid. **13**, 9 (2012).
[9]S.-K. Hoi, Z.-B. Hu, Y. Yan, C.-H. Sow, and A. A. Bettiol, Appl. Phys. Lett. **97**, 183501 (2010).
[10]M. P. MacDonald, G. C. Spalding, and K. Dholakia, Nature **426**, 421 (2003).
[11]C. Helmbrecht, R. Niessner, and C. Haisch, Anal. Chem. **79**, 7097 (2007).
[12]S. J. Hart and A. V. Terray, Appl. Phys. Lett. **83**, 5316 (2003).
[13]S. B. Kim, E. Jung, H. J. Sung, and S. S. Kim, Appl. Phys. Lett. **93**, 044103 (2008).
[14]K. H. Lee, S. B. Kim, K. S. Lee, J. H. Jung, C. B. Chang, and H. J. Sung, Appl. Phys. Lett. **102**, 141911 (2013).

[15]P. Fei, Z. Chen, Y. Men, A. Li, Y. Shen, and Y. Huang, Lab Chip **12**, 3700 (2012).
[16]K. S. Lee, S. Y. Yoon, K. H. Lee, S. B. Kim, H. J. Sung, and S. S. Kim, J. Opt. Soc. Am. B **29**, 407 (2012).
[17]See supplementary material at http://dx.doi.org/10.1063/1.4817938 for Movie S1 showing hollow glass particles flowing in a row.
[18]P. A. Prentice, M. P. MacDonald, T. G. Frank, A. Cuschieri, G. C. Spalding, W. Sibbett, P. A. Campbell, and K. Dholakia, Opt. Express **12**, 593 (2004).